JOURNAL OF GUIDANCE, CONTROL, AND DYNAMICS
Vol. 19, No. 4, July–August 1996

Attitude Control for Low Lift/Drag Re-Entry Vehicles

Alberto Cavallo* and Giuseppe De Maria†
Seconda Università di Napoli, 81031 Aversa (CE), Italy
and
Ferdinando Ferrara‡
Centro Italiano Ricerche Aerospaziali, 81043 Capua (CE), Italy

We propose an attitude control system for a re-entry capsule with a low lift/drag ratio (0.3). The control law is based on quaternions and on a sliding manifold approach. By using the singular perturbation theory, a feedback controller is designed with robustness properties with respect to structural parametric uncertainties and environmental disturbances. The system state remains in a neighborhood of a reference attitude and the control signal is close to the well-defined equivalent control. The reference attitude is commanded by a trajectory controller that steers the vehicle on a reference precalculated path. This controller is based on a time-varying linear quadratic and a variable structure system strategy to meet landing accuracy requirements. Moreover, a new modulator scheme is proposed to modulate the thrust torque commanded by the attitude controller. The overall control law is tested by using a six-degree-of-freedom model of the capsule, taking into account an oblate rotating Earth, and gravitational field, aerodynamics, propulsive forces, and moments. Simulation results show the effectiveness of the proposed control strategy in meeting the requirements on landing accuracy and on heating and load factor limits.

Nomenclature

J = actual inertia matrix
M_a = aerodynamic torque vector
M_t = thrust torque vector
q = quaternion vector
u = control input vector
w = disturbance vector
x = state vector
$\hat{x}$ = reference state vector
α = angle of attack
β = sideslip angle
γ = flight-path angle
θ_L = geocentric longitude
θ_{L0} = initial geocentric longitude
μ = Earth's gravitational constant
σ = bank angle
$\hat{\sigma}$ = reference bank angle
ϕ_L = geocentric latitude
ψ = heading angle
ω = angular rate vector
ω_p = Earth's angular velocity

Introduction

IN view of the foreseen development of the International Space Station, some re-entry vehicles are currently under study. The Space Shuttle Orbiter can be used for normal crew rotation and resupply operations, but, in the case of emergencies, re-entry vehicles can serve as an alternative to the Shuttle to guarantee the return of all or part of the crew members. In fact, to use a Shuttle to evacuate the crew is highly expensive, and moreover the Shuttle may not always be available.

Both in Europe[1] and in the United States,[2] an attractive alternative to the Space Shuttle is being studied: the assured crew re-entry vehicle (ACRV). It is a re-entry vehicle with limited aerodynamics that is easy to refurbish and to carry onboard, but able to land with sufficient accuracy.

Received Aug. 21, 1995; revision received Feb. 15, 1996; accepted for publication Feb. 20, 1996.

*Researcher, Dipartimento di Ingegneria dell'Informazione, Via Roma 29.
†Professor, Dipartimento di Ingegneria dell'Informazione, Via Roma 29.
‡Control Engineer, Flight Mechanics and Control Group, Via Maiorise.

The first results of this study have led to an Apollo-shaped vehicle with a maximum diameter of 4.5 m and a height of 4.6 m, mass of 6000 kg with six crew members, and lift/drag (L/D) ratio of 0.3, obtained with a constant angle of attack of 160 deg (trim value), allowing a cross-range capability of 100 km. The landing accuracy dispersion requirement is 7.6 km, 1σ, at the drogue opening (7-km altitude).

The ACRV re-entry mission is composed of three phases: the retreat, the orbital flight, and the atmospheric phase. The latter is, in turn, decomposed into re-entry, parachute flight, and landing. During the re-entry the capsule must follow a reference trajectory, determined according to terminal path constraints, maximum heating rate, and load factor. In Ref. 3 the problem of the motion of the capsule center of mass has been addressed. More specifically, a trajectory controller has been designed to steer the capsule on the reference path, in the presence of aerodynamic uncertainties, off-nominal initial conditions, and perturbed air density model. The controller designed turns out to be a time-varying linear quadratic (LQ) compensator to control the vehicle in the vertical plane, and a variable structure system (VSS) controller to point the velocity vector toward the target by means of a sequence of roll reversal maneuvers.

In this paper we deal with the problem of the motion of the capsule about the center of mass. More specifically, we propose an attitude controller to track the reference attitude resulting from the trajectory controller. This permits the vehicle to experience the aerodynamic force needed to follow the reference trajectory: the trajectory controller computes the attitude required to follow a desired path, and the attitude controller computes the torques needed to guarantee such an attitude.

To verify the effectiveness of the proposed control strategy, six-degree-of-freedom simulations have been performed, by using the reference trajectory and the path controller designed in Ref. 3. Inertia matrix uncertainties and aerodynamic disturbances are absorbed by the control action.

The attitude controller we propose is based on a sliding manifold approach. Moreover, the large-angle maneuvers in the reference attitude, caused by the roll reversals, prevent us from using Euler angles, which could result in singularity. As a result, quaternions have been used to describe the kinematics.[4] Specifically, given the initial configuration of the vehicle and the reference attitude to track, we design a sliding manifold for which the equivalent control is well defined. By using the singular perturbation theory, a feedback control law is obtained resulting from the solution of a system of differential equations containing a small positive parameter. The closed-loop system exhibits strong robustness properties in spite of structural uncertainties and atmospheric disturbances. Moreover, the system state is in a prescribed neighborhood of the sliding manifold at any time.

Finally, thrusters have been considered to provide the torques required by the attitude controller. Usually, thrusters are modulated by pulse-width and pulse-frequency modulators.[4] We propose a new scheme in which the thrust firing strategy is commanded by a closed-loop modulator which uses a nonlinear device (Schmidt's trigger). This modulator provides an average output torque that equals the required continuous torque profile, commanded by the attitude controller. Moreover, fuel consumption and constraints on minimum on/off time, resulting from the minimum impulse bit (MIB), can be taken into account.

Six-degree-of-freedom simulations including the modulator have shown the effectiveness of the overall control strategy proposed. The simulations have been performed in the presence of both trajectory and attitude disturbances and off-nominal initial conditions.

Coordinate Systems

To describe the model, we must introduce some coordinate systems. The inertial system has the origin at the Earth center, with the X and Y axes in the equatorial plane and the Z axis aligned with the planet polar axis, positive toward the south. The second coordinate system (X_g, Y_g, Z_g) is local geocentric; the Z_g axis is along the line through the center of mass of the body, positive toward the Earth center; the X_g axis is orthogonal to Z_g and positive toward the north, and Y_g completes the right-handed orthogonal frame. The third system we have considered is a body-fixed reference frame (x, y, z), with origin at the vehicle center of mass, the x axis along the geometric longitudinal axis of the body, positive toward the capsule nose, the y axis contained in the symmetry plane of the body pointing downward at entry and perpendicular to the x axis. The z axis completes the right-handed orthogonal frame.

A further coordinate system we have considered is the (X_A, Y_A, Z_A) wind or aerodynamic frame. The X_A axis is along the velocity vector with respect to the local geocentric frame; the drag force is along this axis, with opposite direction; the Z_A axis is aligned with the lift force, with opposite direction; the Y_A axis completes the right-handed orthogonal frame. This frame is defined with respect to the local geocentric system by the flight path angle γ, the heading angle ψ, and the bank angle σ. The wind frame is defined with respect to the body axes by the angle of attack α and that of sideslip β.

The relationships among those reference frames are given by the following rotation matrices. Wind axis coordinates are converted in local geocentric by

$$\begin{pmatrix} X_A \\ Y_A \\ Z_A \end{pmatrix} = \begin{pmatrix} \cos\gamma\cos\psi & \cos\gamma\sin\psi & -\sin\gamma \\ -\sin\psi\cos\sigma + \sin\gamma\cos\psi\sin\sigma & \cos\psi\cos\sigma + \sin\gamma\sin\psi\sin\sigma & \cos\gamma\sin\sigma \\ \sin\psi\sin\sigma + \sin\gamma\cos\psi\cos\sigma & \cos\psi\sin\sigma + \sin\gamma\sin\psi\cos\sigma & \cos\gamma\cos\sigma \end{pmatrix} \begin{pmatrix} X_g \\ Y_g \\ Z_g \end{pmatrix} \tag{1}$$

Inertial coordinates are converted in local geocentric by

$$\begin{pmatrix} X_g \\ Y_g \\ Z_g \end{pmatrix} = \begin{pmatrix} -\sin\phi_L\cos B & -\sin\phi_L\sin B & -\cos\phi_L \\ \sin B & -\cos B & 0 \\ -\cos\phi_L\cos B & -\cos\phi_L\sin B & \sin\phi_L \end{pmatrix} \begin{pmatrix} X \\ Y \\ Z \end{pmatrix} \tag{2}$$

where ϕ_L is the latitude,

$$B = \theta_{L0} - \theta_L - \omega_p t \tag{3}$$

and θ_L and θ_{L0} are the actual and initial longitude, respectively. The conversion between body axes and wind axes is

$$\begin{pmatrix} X_A \\ Y_A \\ Z_A \end{pmatrix} = \begin{pmatrix} \cos\alpha\cos\beta & \sin\beta & \sin\alpha\cos\beta \\ -\sin\beta\cos\alpha & \cos\beta & -\sin\beta\sin\alpha \\ -\sin\alpha & 0 & \cos\alpha \end{pmatrix} \begin{pmatrix} x \\ y \\ z \end{pmatrix} \tag{4}$$

Model

In an inertial reference frame, the rigid-body dynamics equations can be written as

$$\boldsymbol{J}\dot{\boldsymbol{\omega}} + \boldsymbol{S}(\boldsymbol{\omega})\boldsymbol{J}\boldsymbol{\omega} = \boldsymbol{M}_t + \boldsymbol{M}_a \tag{5}$$

where $\boldsymbol{J} = \boldsymbol{J}_0 + \Delta\boldsymbol{J}$ is the actual inertia matrix, $\boldsymbol{J}_0$ is the nominal inertia matrix, $\boldsymbol{\omega} = (\omega_x, \omega_y, \omega_z)^T$ is the vector of angular rates, $\boldsymbol{M}_t$ is the vector of applied thrust torques, $\boldsymbol{M}_a$ is the vector of aerodynamic torques, and the skew-symmetric matrix $\boldsymbol{S}(\boldsymbol{\omega})$ is given by

$$\boldsymbol{S}(\boldsymbol{\omega}) = \begin{pmatrix} 0 & -\omega_z & \omega_y \\ \omega_z & 0 & -\omega_x \\ -\omega_y & \omega_x & 0 \end{pmatrix} \tag{6}$$

Generally, the kinematic description of rigid-body motion involves three parameters known as Euler angles. In the case of large maneuvers, however, the Euler angle description can exhibit singularities. In such cases, an alternative approach is to use quaternions.[5] According to Euler's Theorem, the most general displacement of a rigid body with one point fixed can be defined by a rotation of an angle Φ about some unit vector $\boldsymbol{r}$. We can then define the Euler symmetric parameters

$$\mathbf{q} = \begin{pmatrix} q_1 \\ q_2 \\ q_3 \end{pmatrix} = \boldsymbol{r}\sin\frac{\Phi}{2} \tag{7}$$

$$q_4 = \cos(\Phi/2) \tag{8}$$

and collect them in a quaternion

$$\boldsymbol{q} = \begin{pmatrix} \mathbf{q} \\ q_4 \end{pmatrix} \tag{9}$$

the four elements of the quaternion are not independent but must satisfy the condition

$$q_1^2 + q_2^2 + q_3^2 + q_4^2 = 1 \tag{10}$$

The rigid-body kinematic equation can be shown to be

$$\dot{\boldsymbol{q}} = \tfrac{1}{2}\boldsymbol{\Omega}(\boldsymbol{q})\boldsymbol{\omega} \tag{11}$$

where $\boldsymbol{\Omega}(\boldsymbol{q})$ is the matrix

$$\boldsymbol{\Omega}(\boldsymbol{q}) = \begin{pmatrix} q_4 & -q_3 & q_2 \\ q_3 & q_4 & -q_1 \\ -q_2 & q_1 & q_4 \\ -q_1 & -q_2 & -q_3 \end{pmatrix} \tag{12}$$

Let $\mathcal{B} = \{\boldsymbol{q} \in \boldsymbol{R}^4 : \|\boldsymbol{q}\| = 1\}$ be the unit sphere in $\boldsymbol{R}^4$ and define the state vector $\boldsymbol{x} \in \boldsymbol{R}_1$, where $\boldsymbol{R}_1 = \{\boldsymbol{x} = (\boldsymbol{q}^T, \boldsymbol{\omega}^T)^T \mid \boldsymbol{q} \in \mathcal{B}, \boldsymbol{\omega} \in \boldsymbol{R}^3\}$, the input vector $\boldsymbol{u} = \boldsymbol{M}_t \in \boldsymbol{R}^3$; and the disturbance vector $\boldsymbol{w} = \boldsymbol{M}_a \in \boldsymbol{R}^3$; then we can write

$$\dot{\boldsymbol{x}} = \begin{pmatrix} 0 & \boldsymbol{A}_{12}(\boldsymbol{x}) \\ 0 & \boldsymbol{A}_{22}(\boldsymbol{x}) \end{pmatrix}\boldsymbol{x} + \begin{pmatrix} 0 \\ \boldsymbol{B}_2 \end{pmatrix}\boldsymbol{u} + \begin{pmatrix} 0 \\ \boldsymbol{B}_2 \end{pmatrix}\boldsymbol{w} \tag{13}$$

where $\boldsymbol{A}_{12}(\boldsymbol{x}) = \frac{1}{2}\boldsymbol{\Omega}(\boldsymbol{q})$, $\boldsymbol{A}_{22}(\boldsymbol{x}) = -\boldsymbol{J}^{-1}\boldsymbol{S}(\boldsymbol{\omega})\boldsymbol{J}$, and $\boldsymbol{B}_2 = \boldsymbol{J}^{-1}$.

Attitude Control

Mathematical Background

Consider the system

$$\dot{x} = A(x)x + Bu \tag{14}$$

where $x \in R_1, u \in R^3$, and the map $x \mapsto A(x)$ satisfies a Lipschitz condition on R_1. Let $s : R_1 \times [0, \infty)$ be a continuously differentiable map and define a related sliding manifold as

$$\mathcal{S} = \{(x, t) \in R_1 \times [0, \infty) : s(x, t) = 0\} \tag{15}$$

Consider the function $g(x, u, t) : R_1 \times R^3 \times [0, \infty) \to R^3$ defined by

$$g(x, u, t) = \frac{\partial}{\partial t}s(x, t) + \frac{\partial}{\partial x}s(x, t)[A(x)x + Bu] \tag{16}$$

and for any $\varepsilon > 0$ consider the system of ordinary differential equations

$$\dot{x} = A(x)x + Bu \tag{17}$$

$$\varepsilon\dot{u} = g(x, u, t) \tag{18}$$

Under suitable assumptions of local existence and uniqueness on $\mathcal{S}$ in a suitable neighborhood $\mathcal{I}$ of the manifold,[6] we can give the definition of equivalent control.

Definition 1. For any pair $(x, t) \in \mathcal{I}$, the unique solution $u^*(x, t)$ of the algebraic equation $g(x, u, t) = 0$ is called the equivalent control for the problem

$$\begin{aligned} \dot{x} &= A(x)x + Bu \\ s(x, t) &= 0 \end{aligned} \tag{19}$$

It is possible to show that a necessary and sufficient condition for local existence and uniqueness is that the matrix

$$\frac{\partial}{\partial x}s(x, t)B \tag{20}$$

is not singular for any $(x, t) \in \mathcal{I}$. This condition also defines uniquely the equivalent control as

$$u^*(x, t) = -\left[\frac{\partial}{\partial x}s(x, t)B\right]^{-1}\left[\frac{\partial}{\partial t}s(x, t) + \frac{\partial}{\partial x}s(x, t)A(x)x\right] \tag{21}$$

Moreover, it is required to assure uniform asymptotic stability of the differential equation governing the equivalent control with respect to $(\bar{x}, \bar{t}) \in \mathcal{I}$.

Definition 2. A point $(\bar{x}, \bar{u}, \bar{t})$ such that the solution of the Cauchy problem $\dot{y} = g(\bar{x}, y, \bar{t})$, $y(0) = \bar{u}$, converges asymptotically to $u^*(\bar{x}, \bar{t})$ is said to belong to the domain of influence of $u^*(\bar{x}, \bar{t})$.

The following theorem is a direct consequence of a classic result of the singular perturbation theory.[7] Assuming that conditions for existence and uniqueness of the equivalent control are satisfied and that the origin $x = 0$ of system (17) and (18) corresponding to $\varepsilon = 0$ is exponentially stable, we have the following.

Theorem 1. Let $(x_0, u_0, 0)$ be a point in the domain of influence of $u^*(x_0, 0)$, with $(x_0, 0) \in \mathcal{S}$. Then the solution pair $[x(t, \varepsilon), u(t, \varepsilon)]$ of the Cauchy problem

$$\begin{aligned} \dot{x} &= A(x)x + Bu; & x(0) &= x_0 \\ \varepsilon\dot{u} &= g(x, u, t); & u(0) &= u_0 \end{aligned} \tag{22}$$

has the following properties:

$$\begin{aligned} \lim_{\varepsilon \to 0} x(t, \varepsilon) &= \bar{x}(t) & &\text{uniformly in } [0, \infty) \\ \lim_{\varepsilon \to 0} u(t, \varepsilon) &= \bar{u}(t) & &\text{uniformly in } [t_1, \infty) \end{aligned} \tag{23}$$

for any $t_1 > 0$, and $[\bar{x}(t), \bar{u}(t)]$ is the solution of the reduced system

$$\begin{aligned} \dot{x} &= A(x)x + Bu; & x(0) &= x_0 \\ g(x, u, t) &= 0 \end{aligned} \tag{24}$$

Problem Formulation

Let $\hat{x} = (\hat{q}^T, \hat{\omega}^T)^T \in R_1$ be a reference state attitude that the body is required to follow. Then the tracking problem can be stated as follows: given $\beta > 0$ and $\delta > 0$ and any initial state $x_0 = (q_0^T, \omega_0^T)^T$, it is required to design a feedback control law such that the error vector $e = \hat{x} - x$ satisfies

$$\|e\| \leq \delta + Ae^{-\beta t} \tag{25}$$

for any $t \geq 0$, where A is a constant depending on the data. To solve the attitude tracking problem, we define $s : R_1 \times [0, \infty) \to R^3$ as follows:

$$s(x, t) = H(q)[\hat{x} - x - f(x_0, t)] \tag{26}$$

where $x_0 = x(0), H(q)$ is a matrix of suitable dimensions to be chosen later, and $f(x_0, t)$ is a vector such that

$$f(x_0, 0) = \hat{x}(0) - x_0 \tag{27}$$

and

$$\lim_{t \to \infty} f(x_0, t) = 0 \tag{28}$$

Now consider the system

$$\dot{x} = \begin{pmatrix} 0 & A_{12}(x) \\ 0 & A_{22}(x) \end{pmatrix} x + \begin{pmatrix} 0 \\ B_2 \end{pmatrix} u + \begin{pmatrix} 0 \\ B_2 \end{pmatrix} w \tag{29}$$

$$\varepsilon\dot{u} = g(x, u, t) \tag{30}$$

where g is defined by means of Eqs. (16) and (26). Since $s(x_0, 0) = 0$, the solution $[\bar{x}(t), \bar{u}(t)]$ of the reduced system defined in Theorem 1 satisfies $s[\bar{x}(t), t] = 0$ for any $t \in [0, \infty)$.

Now we let

$$H(q) = [H_1(q) \quad H_2] \tag{31}$$

where $H_1(q) \in R^{3\times 4}$ and H_2 is a full rank 3×3 constant matrix to be chosen. According to Eq. (20) it is easy to prove that existence and uniqueness assumption on the equivalent control holds if and only if the matrix

$$\Gamma = H_2 J^{-1} \tag{32}$$

is nonsingular. Since the inertia matrix, even in the presence of uncertainties, does not lose rank, it is easy to select the matrix H_2 in such a way that Γ has all of the eigenvalues in the right half-plane, to satisfy also the stability assumption referred to in Definition 2.

The matrix $H_1(q)$ can be selected as follows:

$$H_1(q) = H_1' \Omega^T(q) \tag{33}$$

where H_1' is a constant 3×3 matrix. Finally, a possible choice of the function $f(x_0, t)$ satisfying Eq. (27), Eq. (28) is

$$f(x_0, t) = e^{Ct}(\hat{x}_0 - x_0) \tag{34}$$

where C is a stability matrix. Now we can state the following.

Theorem 2. Let $x_0 \in R_1$ be given. Assume that

$$\mathrm{Re}\lambda_{\min}\left(H_2 J^{-1}\right) > 0 \tag{35}$$

and H_1' be a matrix such that $H_2^{-1}H_1'$ is symmetric and positive definite. Let

$$\mathrm{Re}\lambda_{\max}(C) < -\lambda_{\min}\left(H_2^{-1}H_1'\right) \tag{36}$$

Then there exists an $\varepsilon_0 > 0$ such that for any $\varepsilon \in (0, \varepsilon_0]$ the solution $[x(t, \varepsilon), u(t, \varepsilon)]$ to Eqs. (29) and (30) satisfying $[x(0, \varepsilon), u(0, \varepsilon)] = (x_0, u_0)$ is such that

$$|\hat{x}(t) - x(t, \varepsilon)| < \delta + Ae^{-\beta t} \tag{37}$$

with

$$u(t,\varepsilon) = (1/\varepsilon)\left[H_1'\Omega^T(q) \quad H_2\right] \times \left[\hat{x}(t) - x(t,\varepsilon) - e^{Ct}(\hat{x}_0 - x_0)\right] + u_0 \tag{38}$$

where $t \geq 0$ and A and β are positive constants depending on H_1', H_2, C, and x_0.

The proof of Theorem 2 is detailed in the Appendix.

The role of the term $f(x_0, t) = e^{Ct}(\hat{x}_0 - x_0)$ is to slow down the convergence of the error, due to initial off-nominal conditions. The closer to zero the real part of the eigenvalues of C, the slower the convergence of the error will be. Moreover, according to the singular perturbation theory, the smaller that we set ε, the closer the actual state is to the reduced-order model state and the actual control to the equivalent control. This allows us to consider bounds on the control. In fact, by Theorem 1 the control signal $u(t, \varepsilon)$ approaches the equivalent control $\tilde{u}(t)$, and the shape of the equivalent control is determined by the matrix C and by the reference trajectory. It is possible to show that the equivalent control is given by

$$u^* = J\left[\dot{\omega} + C_\omega e^{C_\omega t}(\hat{\omega}_0 - \omega_0)\right] + S\left[\hat{\omega} + e^{C_\omega t}(\hat{\omega}_0 - \omega_0)\right] \times J\left[\hat{\omega} + e^{C_\omega t}(\hat{\omega}_0 - \omega_0)\right] - M_a \tag{39}$$

Then we can select the nominal trajectory and the term $e^{Ct}(\hat{x}_0 - x_0)$ to fulfill bounds on the equivalent control and select ε small enough to guarantee that the actual control does not violate these bounds. Moreover, the presence of the term $e^{Ct}(\hat{x}_0 - x_0)$ avoids the drawbacks of high gain control systems such as peaking phenomena. Finally, note that the equivalent control input (39) absorbs both the inertia matrix uncertainties and the aerodynamic disturbances, as evidenced by the equations of the reduced-order system (A8) and (A9) in the Appendix.

Attitude Control for Low *L/D* Re-Entry Vehicles

The problem of steering a capsule along a prescribed trajectory has been addressed in Ref. 3. In that paper we considered the linearized model of the capsule along a nominal trajectory, obtained by means of an optimization code that minimized the total thermal load taking into account path constraints on the load factor, maximum stagnation point heating rate, and terminal path constraints, assuring a nominal 100-km cross range. The control strategy assumed fixed angles of attack $\alpha = 160$ deg and sideslip $\beta = 0$ deg, whereas the bank angle σ is used as control variable. This strategy involves a feedback on altitude, relative speed, flight-path angle and range to go.

Then a time-varying LQ controller was designed to follow the trajectory in the vertical plane in spite of aerodynamic disturbances and structural uncertainties. Since the vertical plane motion is not affected by the sign of the bank angle, a VSS strategy was employed to point the vehicle velocity vector toward the target. The heading angle error used in this feedback loop was deduced from the actual heading angle, latitude and longitude, and from the target latitude and longitude. This strategy resulted in a sequence of roll reversal maneuvers.

The control law in Ref. 3 has proved to be robust against off-nominal initial conditions, aerodynamic coefficient uncertainties, and air density perturbations. The result of the paper are three commanded angles α_c, β_c, and σ_c that the actual angles α, β, and σ are required to follow.

In this paper an attitude controller is designed to accomplish such a task. In Ref. 3 sudden roll reversal maneuvers have been assumed. Since this assumption is not realistic and would generate impulsive attitude reference profiles, a filter has been added to smooth the bank angle. The filter should avoid wide overshoot and oscillations. A possible solution is an ITAE filter, whose coefficients are computed to minimize the integral of the product of time and absolute values of an error to a step. A second-order ITAE filter $F(s)$ assuring 12-s rise time has been used.

Obviously, the filter action decreases the performances of the trajectory controller, nevertheless trajectory simulations carried on in the presence of such a filter show that ground dispersion requirements are still met. Thus, the trajectory controller generates, at each time instant, a continuously differentiable reference trajectory $[\hat{\alpha}(t), \hat{\beta}(t), \hat{\sigma}(t)]$ to track. This trajectory must be converted into reference quaternions and reference angular rates. This can be achieved by using Eqs. (1–4) to compute the 3×3 direction cosine matrix E that defines the orientation of the body axes with respect to the inertial frame. To compute the matrix E, the variables γ, ψ, θ_L, and ϕ_L are supplied by the navigation system. The quaternions are computed as[5]

$$\hat{q}_4 = \pm\tfrac{1}{2}\sqrt{1 + e_{11} + e_{22} + e_{33}} \tag{40}$$

$$\hat{q}_1 = (1/4q_4)(e_{23} - e_{32}) \tag{41}$$

$$\hat{q}_2 = (1/4q_4)(e_{31} - e_{13}) \tag{42}$$

$$\hat{q}_3 = (1/4q_4)(e_{12} - e_{21}) \tag{43}$$

Equation (40) evidences the well-known fact that quaternions with the same absolute value and opposite sign, q and $-q$, describe the same orientation. Since the sign ambiguity in Eq. (40) could result in discontinuous reference trajectories, the sign in Eq. (40) must be selected at each time instant to ensure a continuous quaternion reference trajectory.

Furthermore, by using Eq. (11), the reference angular velocity can be computed:

$$\hat{\omega} = 2\Omega(\hat{q})^T \dot{\hat{q}} \tag{44}$$

where $\dot{\hat{q}}$ is numerically computed by using a high-pass filter $H(s)$.

The actual quaternions and angular velocities, as well as all of the position and velocity variables required to generate the reference quaternions, are provided by the navigation system. The complete attitude and trajectory control scheme is depicted in Fig. 1. The values of the inertia moments of the capsule are

$$J_{xx} = 8889, \qquad J_{yy} = J_{zz} = 12{,}015$$
$$J_{xy} = J_{xz} = J_{yz} = 0 \text{ kg} \cdot \text{m}^2 \tag{45}$$

The ITAE filter is

$$F(s) = \frac{1}{36s^2 + 8.484s + 1} \tag{46}$$

The high-pass filter is

$$H(s) = \frac{100s}{s + 100} \tag{47}$$

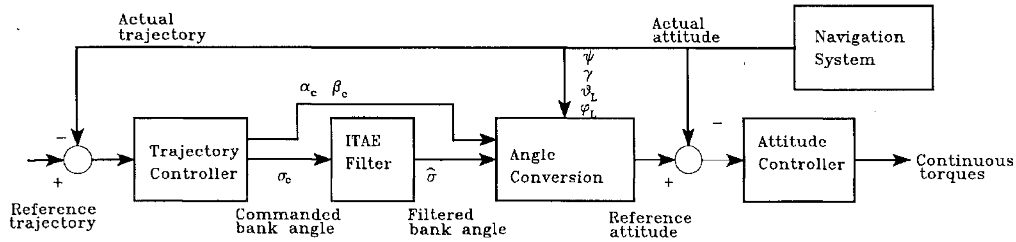

Fig. 1 Complete control scheme.

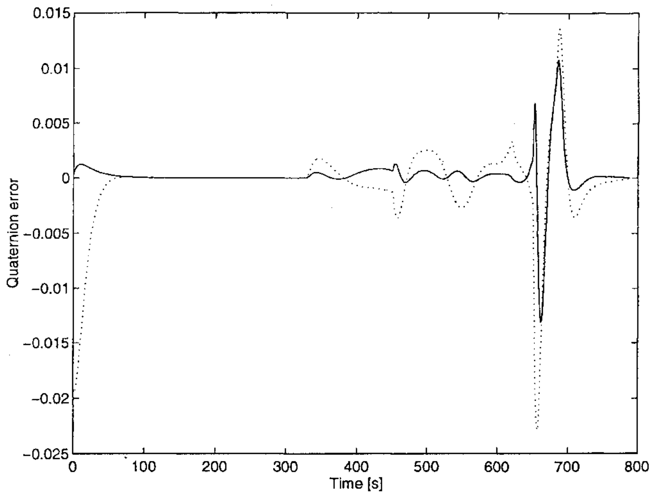

Fig. 2 Quaternions q_1 and q_2 tracking errors: ——, q_1 error and ·····, q_2 error.

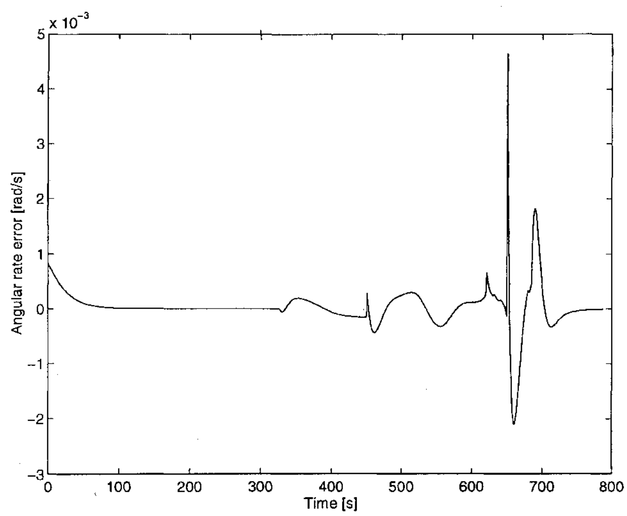

Fig. 3 Angular velocity ω_x error.

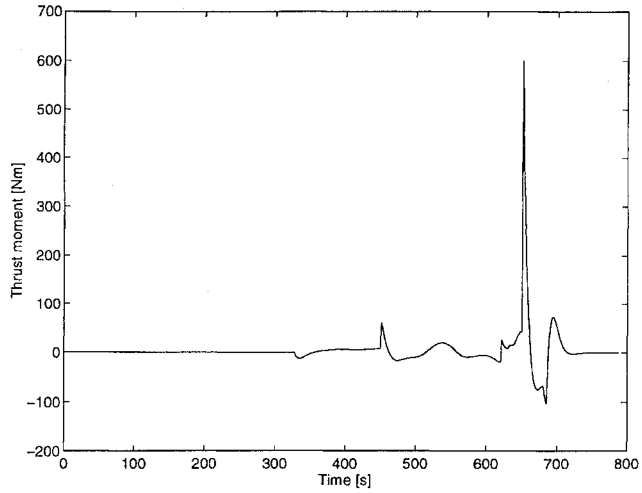

Fig. 4 Control torque M_x.

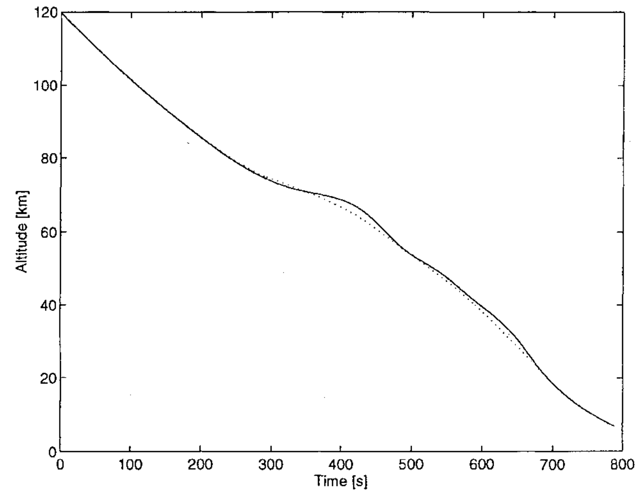

Fig. 5 Geodetic altitude behavior: ——, actual trajectory and ·····, nominal trajectory.

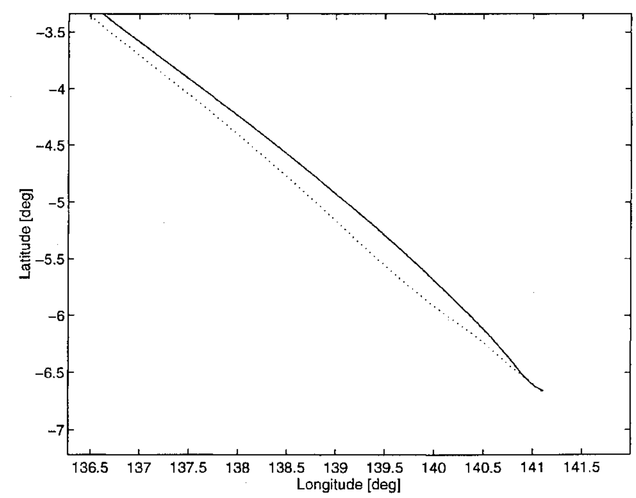

Fig. 6 Ground track: ——, actual trajectory and ·····, nominal trajectory.

The matrices in Theorem 2 have been selected as

$$H_1' = 10I_3, \qquad H_2 = \mathrm{diag}(100, 50, 50) \tag{48}$$

$$C = \mathrm{diag}(C_q, C_\omega) \tag{49}$$

$$C_q = -0.1I_4, \qquad C_\omega = -0.1I_3 \tag{50}$$

The matrix C is selected to recover off-nominal initial condition in about 50 s, and $\varepsilon = 0.001$.

An initial conditions mismatch has been assumed:

$$\begin{aligned} \hat{q}_0 &= (0.7272, 0.1207, -0.6426, -0.2091) \\ q_0 &= (0.7268, 0.14, -0.6274, -0.2419) \end{aligned} \tag{51}$$

$$\hat{\omega}_0 = (0.0008, 0.001, -0.002), \qquad \omega_0 = (0, 0, 0) \tag{52}$$

Simulations have been carried out in the presence of aerodynamic disturbance torques and 2% inertia matrix uncertainties with a six-degree-of-freedom simulation code. Trajectory perturbations and off-nominal initial conditions have been considered according to the numerical values in Ref. 3.

The results are shown in Figs. 2–4. In Fig. 2 the quaternion tracking errors e_{q_1} and e_{q_2} are reported. In Fig. 3 the behavior of the angular rate error e_{ω_x} is depicted. In Fig. 4 the x-axis control torque is shown. Note the high peak required by the roll-reversal maneuver. The geodetic altitude-time history and the last 340 s of the ground track history are presented in Figs. 5 and 6, respectively.

Finally, the problem of control implementation has been addressed. The actuators we used are hydrazine thrusters.[8] The commanded control and its derivative resulting from our strategy are continuous, whereas the actual control operates in pulse mode; moreover, the MIB phenomenon determines minimum on and off time. The modulator scheme we propose is depicted in Fig. 7. In this scheme, the presence of the feedback loop and the integrator

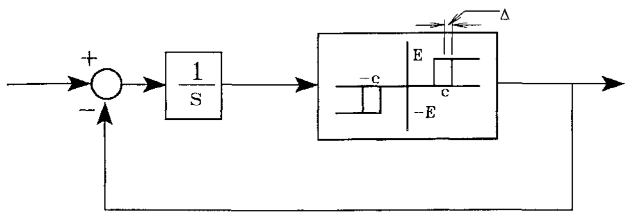

Fig. 7 Modulator scheme.

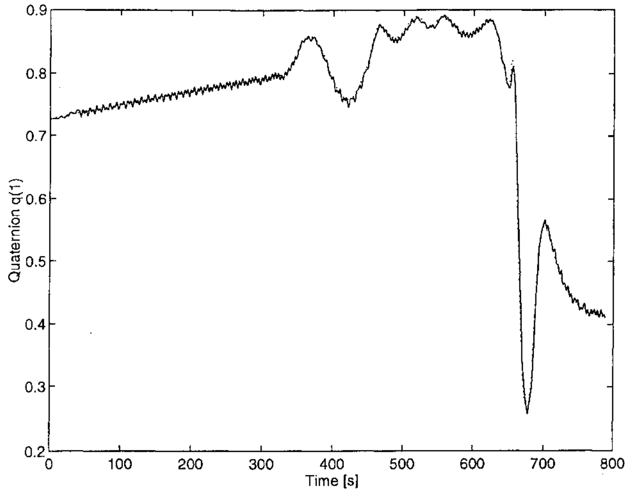

Fig. 8 Quaternion q_1 tracking with thrusters: ——, actual and ·····, reference.

guarantees that the mean value of the modulated output follows the continuous input signal, whereas the nonlinear device (Schmidt's trigger) takes into account fuel consumption and MIB. More specifically, the parameters of the trigger are chosen as follows: the amplitude E of the trigger must be larger than the maximum value of the commanded torque, to assure stability of the scheme. The hysteresis shift c is related to the largest admissible tracking error; the hysteresis amplitude 2Δ takes into account the MIB. The amplitude of the torque values are selected according to the largest values of the equivalent control for each axis. Moreover, the larger the dead zone the lower the fuel consumption. Therefore, the width of the dead zone must be selected to assure a good compromise between both tracking error and fuel consumption. However, the tracking error is also influenced, as already seen, by the parameter ε, whose value must be selected to take into account the tracking error due to the dead zone.

This scheme can be seen as a modification of the pulse ratio modulator[9,10] and retains the same stability and mean value properties,[11] as can be proved by using the VSS theory.[12] This modulator guarantees that the mean value of the actual thrust moment follows, up to an error controlled by the width of the dead zone, the continuous control required by our attitude control strategy. Because of the large values of the inertia matrix, the capsule works like a narrow low-pass filter, cutting off the high-frequency components of the actual control.

The parameters of the modulator have been chosen as follows:

$$E_x = 800\,\mathrm{N\cdot m}, \qquad c_x = 400\,\mathrm{N\cdot m\cdot s} \qquad \Delta_x = 200\,\mathrm{N\cdot m\cdot s} \tag{53}$$

$$E_y = 200\,\mathrm{N\cdot m}, \qquad c_x = 100\,\mathrm{N\cdot m\cdot s} \qquad \Delta_x = 50\,\mathrm{N\cdot m\cdot s} \tag{54}$$

$$E_x = 400\,\mathrm{N\cdot m}, \qquad c_x = 200\,\mathrm{N\cdot m\cdot s} \qquad \Delta_x = 100\,\mathrm{N\cdot m\cdot s} \tag{55}$$

Moreover, a larger value $\varepsilon = 0.005$ has been imposed to guarantee feasible control consumption and minimum on time.

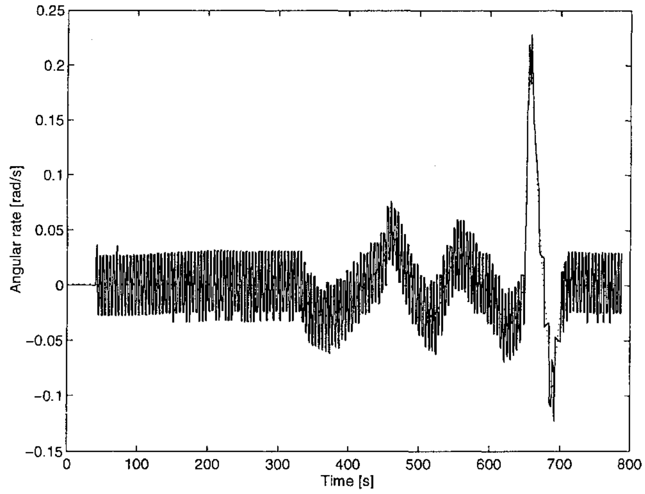

Fig. 9 Angular velocity ω_x tracking with thrusters: ——, actual and ·····, reference.

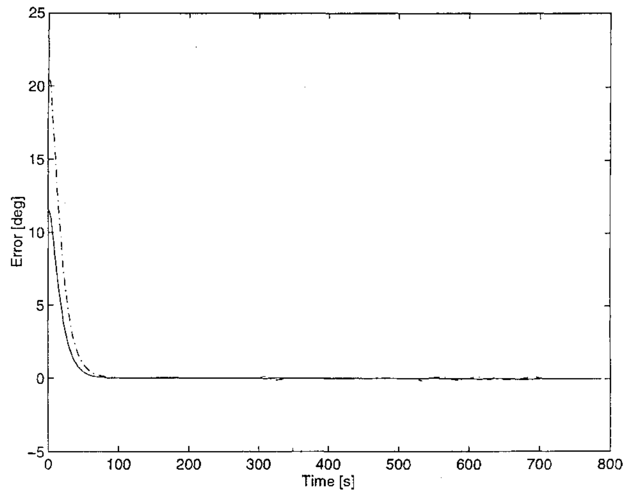

Fig. 10 Angles α and β errors: ——, α error and · – · –, β error.

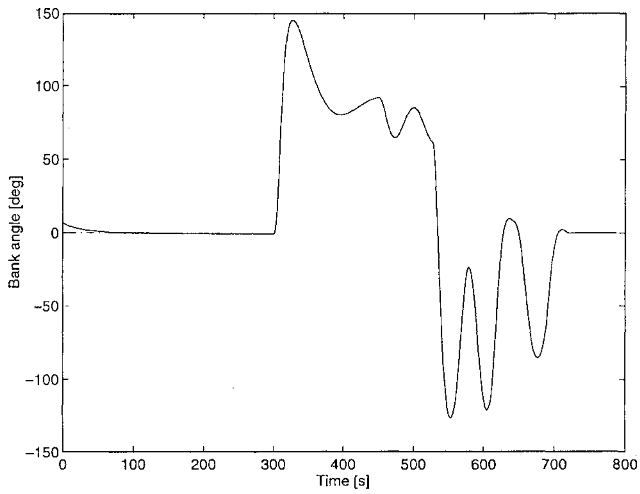

Fig. 11 Actual and commanded bank angle: ——, actual and · – · –, commanded.

The simulations performed with actuator are shown in Figs. 8 and 9. Obviously, the larger value for ε and the width of the dead zones result in decreased tracking performances, as evidenced in Fig. 8.

Comparison with the results in Ref. 3 shows the effectiveness of the proposed technique. In Fig. 10, α and β errors are shown, whereas the bank angle σ is depicted in Fig. 11.

Conclusions

In this paper an attitude control system for a re-entry capsule has been proposed. A reference attitude profile is obtained from a trajectory controller, converted in reference quaternions and angular rates, and tracked by the capsule. The attitude control law is based on a sliding manifold approach and on the theory of singular perturbations.

Thrust torques are modulated by a new modulator, able to take into account fuel consumption and minimum on/off time. Simulations are performed by a six-degree-of-freedom code, taking into account structural uncertainties and environmental disturbances.

Appendix: Proof of Theorem 2

To prove the theorem we must preliminarily recall some properties of the quaternion representation. For any $\boldsymbol{q}_1, \boldsymbol{q}_2 \in \mathcal{B}$, we have

$$\boldsymbol{\Omega}^T(\boldsymbol{q}_1)\boldsymbol{q}_2 = -\boldsymbol{\Omega}^T(\boldsymbol{q}_2)\boldsymbol{q}_1 \tag{A1}$$

Moreover, for any $\boldsymbol{q} \in \mathcal{B}$,

$$\boldsymbol{\Omega}^T(\boldsymbol{q})\boldsymbol{q} = \boldsymbol{0} \tag{A2}$$

$$\boldsymbol{\Omega}^T(\boldsymbol{q})\boldsymbol{\Omega}(\boldsymbol{q}) = \boldsymbol{I}_3 \tag{A3}$$

Finally, two coordinate frames with quaternion representation $\boldsymbol{p}$ and $\boldsymbol{q}$ coincide[13,14] if and only if $\delta\boldsymbol{q} = 0$, where

$$\delta\boldsymbol{q} = q_4\,\mathbf{p} - p_4\mathbf{q} - \boldsymbol{S}(\mathbf{q})\mathbf{p} \tag{A4}$$

and the operator $\boldsymbol{S}(\cdot)$ is defined in Eq. (6).

Now we are ready to prove the theorem. We define the tracking error $\boldsymbol{e} = \hat{\boldsymbol{x}} - \boldsymbol{x}$ and apply Theorem 1 to the error dynamics. The tracking error can be split into two components:

$$\boldsymbol{e} = \begin{pmatrix} \boldsymbol{e}_q \\ \boldsymbol{e}_\omega \end{pmatrix} \tag{A5}$$

Letting $\boldsymbol{f} = (\boldsymbol{f}_1^T \; \boldsymbol{f}_2^T)^T$ and computing the function $\boldsymbol{g}(\boldsymbol{x}, \boldsymbol{u}, t)$ as in Eq. (16) we have

$$\dot{s} = [\boldsymbol{H}_1(\dot{\boldsymbol{q}}) \quad \boldsymbol{0}]\left[\begin{pmatrix} \boldsymbol{e}_q \\ \boldsymbol{e}_\omega \end{pmatrix} - \begin{pmatrix} \boldsymbol{f}_1 \\ \boldsymbol{f}_2 \end{pmatrix}\right] + [\boldsymbol{H}_1(\boldsymbol{q}) \quad \boldsymbol{H}_2]\left[\begin{pmatrix} \dot{\boldsymbol{e}}_q \\ \dot{\boldsymbol{e}}_\omega \end{pmatrix} - \begin{pmatrix} \dot{\boldsymbol{f}}_1 \\ \dot{\boldsymbol{f}}_2 \end{pmatrix}\right] \tag{A6}$$

By using property (A1) it is easy to compute the equivalent control

$$\boldsymbol{u}^* = \left(\boldsymbol{H}_2\boldsymbol{J}^{-1}\right)^{-1}\left[\boldsymbol{H}_1(\tilde{\boldsymbol{q}})\dot{\hat{\boldsymbol{q}}} - \boldsymbol{H}_1(\hat{\boldsymbol{q}})\dot{\tilde{\boldsymbol{q}}} + \boldsymbol{H}_1(\boldsymbol{f}_1)\dot{\tilde{\boldsymbol{q}}} - \boldsymbol{H}_1(\tilde{\boldsymbol{q}})\dot{\boldsymbol{f}}_1 + \boldsymbol{H}_2\dot{\hat{\boldsymbol{\omega}}} + \boldsymbol{H}_2\boldsymbol{J}^{-1}\boldsymbol{B}(\tilde{\boldsymbol{\omega}})\boldsymbol{J}\tilde{\boldsymbol{\omega}} - \boldsymbol{H}_2\dot{\boldsymbol{f}}_2\right] - \boldsymbol{M}_a \tag{A7}$$

The solution $\tilde{\boldsymbol{\omega}}$ of the reduced-order system is

$$\tilde{\boldsymbol{\omega}}(t) = \hat{\boldsymbol{\omega}}(t) - \boldsymbol{f}_2 + \boldsymbol{H}_2^{-1}\boldsymbol{H}_1(\tilde{\boldsymbol{q}})\hat{\boldsymbol{q}} - \boldsymbol{H}_2^{-1}\boldsymbol{H}_1(\tilde{\boldsymbol{q}})\boldsymbol{f}_1 \tag{A8}$$

where $\tilde{\boldsymbol{q}}$ is governed by the differential equation

$$\dot{\tilde{\boldsymbol{q}}} = \tfrac{1}{2}\boldsymbol{\Omega}(\tilde{\boldsymbol{q}})\tilde{\boldsymbol{\omega}} \tag{A9}$$

Note that, according to Eq. (A8) and by using Eqs. (33), (A2), and (34), if the quaternion error converges to zero, the angular rate error $\tilde{\boldsymbol{e}}_\omega$ also vanishes. To test the convergence of the quaternion error, we choose as a Lyapunov function

$$V = \tilde{\boldsymbol{e}}_q^T\tilde{\boldsymbol{e}}_q \tag{A10}$$

Computing the time derivative of the Lyapunov function along the trajectory defined by Eq. (A9) and the reference trajectory

$$\dot{\hat{\boldsymbol{q}}} = \tfrac{1}{2}\boldsymbol{\Omega}(\hat{\boldsymbol{q}})\hat{\boldsymbol{\omega}} \tag{A11}$$

we have

$$\dot{V} = -\delta\tilde{\boldsymbol{q}}^T\boldsymbol{H}_2^{-1}\boldsymbol{H}_1'\delta\tilde{\boldsymbol{q}} + \delta\tilde{\boldsymbol{q}}^T\boldsymbol{H}_2^{-1}\boldsymbol{H}_1\boldsymbol{f}_1 + \delta\tilde{\boldsymbol{q}}^T\boldsymbol{H}_2^{-1}\boldsymbol{H}_1\boldsymbol{f}_2 \tag{A12}$$

where $\delta\tilde{\boldsymbol{q}}$, defined by Eq. (A4), can be shown to be

$$\delta\tilde{\boldsymbol{q}} = \boldsymbol{\Omega}^T(\tilde{\boldsymbol{q}})\hat{\boldsymbol{q}} \tag{A13}$$

then if $\boldsymbol{H}_2^{-1}\boldsymbol{H}_1'$ has been selected to be positive definite, there exists $t^* > 0$ such that $\dot{V} < 0$, $\forall t \geq t^*$. As in the interval $[0, t^*]$ the quaternion error is bounded, $\|\boldsymbol{e}_q\| = \|\hat{\boldsymbol{q}} - \tilde{\boldsymbol{q}}\| \leq 2$, we have

$$\lim_{t\to\infty} \tilde{\boldsymbol{e}}_q(t) = 0 \tag{A14}$$

Finally, applying Theorem 1 to the tracking error we complete the proof.

References

[1]Jallade, S., and Champetier, C., "Assured Crew Return Vehicle GNC Design," Matra Marconi Space, ACRV/RT/SJ/38.92, 1993.

[2]Reding, J. P., and Svendsen, H. O., "Lifting Entry Rescue Vehicle Configuration," *Journal of Spacecraft and Rockets*, Vol. 27, No. 5, 1990, pp. 606–612.

[3]Cavallo, A., and Ferrara, F., "Atmospheric Reentry Control for Low Lift/Drag Vehicles," *Journal of Guidance, Control, and Dynamics*, Vol. 19, No. 1, 1996, pp. 47–53.

[4]Vadali, S. R., "Variable-Structure Control of Spacecraft Large-Angle Maneuver," *Journal of Guidance, Control, and Dynamics*, Vol. 9, No. 2, 1986, pp. 235–239.

[5]Wertz, J., *Spacecraft Attitude Determination and Control*, Reidel, Dordrecht, The Netherlands, 1986.

[6]Cavallo, A., De Maria, G., and Nistri, P., "Some Control Problems Solved via a Sliding Manifold Approach," *Differential Equations and Dynamical Systems*, Vol. 1, No. 4, 1993, pp. 295–310.

[7]Wasow, W., *Asymptotic Expansions for Ordinary Differential Equations*, Wiley-Interscience, New York, 1965.

[8]Cavallo, A., De Maria, G., and Marino, P., "Simulation Model for Catalytic Monopropellant Hydrazine Thruster," *Proceedings of the IFAC Symposium on Intelligent Components and Instruments for Control Applications*, Malaga, Spain, 1992, pp. 669–672.

[9]De Maria, G., and Sciavicco, L., "Analysis and Design of Pulse Ratio Modulated Feedback Control Systems," *IEEE Transactions on Industrial Electronics and Control Instrumentation*, Vol. 26, No. 3, 1979, pp. 166–172.

[10]Schaffer, R. A., "A New Pulse Modulator for Accurate DC Amplifications with Linear or Nonlinear Devices," *IRE Transactions on Instrumentation*, Vol. 11, No. 2, 1962, pp. 34–47.

[11]Cavallo, A., and Vasca, F., "DC Motor Control with Sliding Mode Switching Modulator," *IEEE Conference on Industrial Electronics, Control, and Instrumentations* (Bologna, Italy), 1994, pp. 1455–1459.

[12]Utkin, V. I., *Sliding Modes in Control and Optimization*, Springer–Verlag, Berlin, 1991.

[13]Yuan, J. S.-C., "Closed-Loop Manipulator Control Using Quaternion Feedback," *IEEE Journal of Robotics and Automation*, Vol. 4, No. 4, 1988, pp. 434–440.

[14]Paielli, R. A., and Bach, R. E., "Attitude Control with Realization of Linear Error Dynamics," *Journal of Guidance, Control, and Dynamics*, Vol. 16, No. 1, 1993, pp. 182–189.